

Hybrid Digital Twins: A Proof of Concept for Reinforced Concrete Beams

Max von Danwitz^{1,*}, Thank Thank Kochmann¹, Tarik Sahin¹, Johannes Wimmer², Thomas Braml², and Alexander Popp¹

¹ Institute for Mathematics and Computer-Based Simulation (IMCS),

University of the Bundeswehr Munich, Werner-Heisenberg-Weg 39, D-85577 Neubiberg, Germany

² Institute for Structural Engineering,

University of the Bundeswehr Munich, Werner-Heisenberg-Weg 39, D-85577 Neubiberg, Germany

Digital twins map physical objects, processes, and further entities from the real (physical) world into digital space. Going one step further, hybrid digital twins combine physics-based modeling with data-based techniques to form a simulation tool with predictive power. In the light of an increasing digitalization of our built world, such digital twins have great potential to contribute to the protection of critical technical infrastructures. In case of bridges, digital twins can have a key role in structural health monitoring. This contribution outlines a path to approach these goals and provides a proof of concept of a hybrid digital twin for steel-reinforced concrete beams as a representative component in civil engineering structures.

Four model components are combined to form the hybrid digital twin, namely, a physics-based full-order model, a fast-to-evaluate reduced-order model, a purely data-driven model, and a baseline model. Applied to the concrete beam, the full-order model is based on a novel finite element formulation allowing for efficient modeling of slender structures embedded into solid bodies. We use this method to capture the interaction between reinforcement components and concrete matrix of the beam. As reduced-order model, a physics-informed neural network is trained with parts of the available measurement data and with the governing equations of a simplified physical model. The data-driven model localizes cracks in the concrete in a statistical outlier analysis of fiber-optical strain measurement data. In completion, the baseline model estimates the system behavior based on a closed-form expression from civil engineering literature.

The proposed hierarchy of four models with decreasing model complexity allows to select an appropriate model according to an application specific trade-off between model accuracy and cost. We demonstrate the combination of physics-based modeling with data-driven techniques based on sensor data measured in a physical four-point bending test of the reinforced concrete beam.

© 2023 The Authors. *Proceedings in Applied Mathematics & Mechanics* published by Wiley-VCH GmbH.

1 Introduction

Critical infrastructures are the lifelines of modern society. For example, highway and railroad bridges are indispensable for ensuring reliable public and private transport. In Germany, concrete bridges provide 88% of the total area of bridges on federal highways. Moreover, approximately 50% of these bridges were built before 1980 and require regular inspection [1]. In the field of structural health monitoring (SHM), sensor-based digital representations of bridges are explored to reduce the number of expensive on-site inspections. In particular, digital twins have great potential in SHM and predictive maintenance of bridges [2].

The term digital twin was coined in the context of manufacturing, however, the concept is also explored in various other fields such as health care, education, meteorology and construction [3]. From a general point of view, *digital twins* map physical objects, processes, and further entities from the real (physical) world into digital space. For an overview of the research on digital twins we refer to the recent review paper of Rasheed et al. [3]. The authors provide a broad perspective on models for digital twins and discuss high fidelity numerical simulators, data-driven modeling, and reduced-order modeling as enabling technologies for digital twins.

In the following, we focus on digital twins that model an underlying physical problem which is described by partial differential equations (PDE) (Section 2). In particular, we develop a *hybrid digital twin* that combines physics-based modeling with data-based techniques to form a simulation tool with predictive power. The process of generating a hybrid digital twin is termed *hybrid digital twinning*. Inputs for this process include drawings, designs, Computer-Aided Design (CAD) geometries of the physical system under consideration. Material properties are assumed to be known from literature or characterized by experiments. To interact with its digital representation, the real system is expected to provide sensor data which may, e.g., include strain measurements on the surface and in the interior with embedded sensors, displacements, accelerations, and temperatures.

The application case of a reinforced concrete beam, presented in Section 3, brings us back to our motivation of concrete bridges as we strive for a reliable digital representation of steel-reinforced concrete structures for damage detection. In Section 4, we test the hybrid digital twin of a reinforced concrete beam with measurement data of a four-point bending test performed in a physical experiment. Finally, Section 5 offers conclusion and outlook.

* Corresponding author: e-mail max.danwitz@unibw.de, phone +49 89 6004 4628, fax +49 89 6004 4136



This is an open access article under the terms of the Creative Commons Attribution License, which permits use, distribution and reproduction in any medium, provided the original work is properly cited.

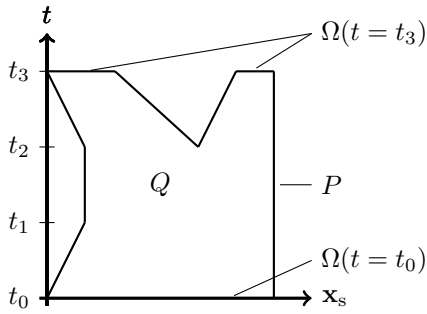


Fig. 1: Spatial domain Ω and space-time domain Q [4].

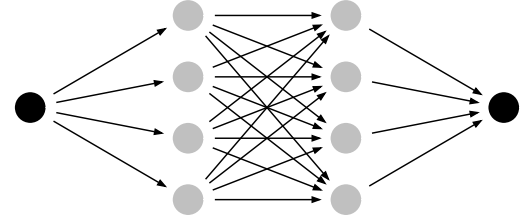


Fig. 2: Feed-forward neural network with two hidden layers.

2 Models and Methods for Hybrid Digital Twins

A central requirement for a hybrid digital twin is an accurate description of the real physical system. Such an accurate description can be provided by high fidelity numerical simulators, e.g., finite element models [3]. Response times for individual evaluations of a complex simulator can range from a few minutes to hours or even beyond. However, in digital twin applications that require many queries, e.g., uncertainty quantification, or real-time(-like) applications, e.g., control problems a fast-response time is essential. In such cases, the response time of a high fidelity simulator becomes prohibitively expensive and a trade-off between model accuracy and response time is required.

To allow for an application specific trade-off between accuracy and response time, we propose a hybrid digital twin that has four components:

- a full-order model (FOM) that provides a detailed understanding of the physical behavior,
- a reduced-order model (ROM) that is fast to evaluate and can interact with sensor data,
- a data-driven model (DDM) obtaining insight into the system state based on statistical analysis of sensor data, and
- a baseline model (BLM) that provides an engineering estimate for the modeled system behavior.

FOM, ROM, and BLM are derived from a mathematically formulated physical model of the real system. Therefore, Section 2.1 presents a PDE-based initial boundary value problem (IBVP) as starting point for the model derivation. As ROM we consider a physics-informed neural network (PINN). Subsequently, Section 2.2 outlines the derivation of a PINN formulation for a general IBVP. In contrast, FOM, DDM, and BLM are based on more established methods which are introduced directly in the context of the application case in Section 3.

2.1 Physics-based Modeling of Time-Dependent Problems

We consider a PDE for a vector-valued function \mathbf{u} with n_{df} independent variables. For convenience, the PDE is expressed in residual form, i.e., $\mathcal{R}(\mathbf{u}) = \mathbf{0}$, with $\mathcal{R}: \mathbb{R}^{n_{df}} \rightarrow \mathbb{R}^{n_{df}}$. Furthermore, the model problem requires the PDE to hold on a spatial computational domain $\Omega(t) \subset \mathbb{R}^{n_{sd}}$ and over a time interval $I = [0, t_f]$. As indicated in Figure 1, the temporal evolution of Ω generates the space-time continuum Q , and the evolution of the spatial domain boundary results in a space-time boundary P . Points in the domain are characterized by the spatial coordinates $\mathbf{x}_s \in \mathbb{R}^{n_{sd}}$ and the time coordinate t . For a three-dimensional spatial problem, the spatial coordinates are collected in a vector $\mathbf{x}_s = [x, y, z]^T$.

With these definitions, we can formulate the underlying physical model as IBVP. On the computational space-time domain Q , we seek the solution $\mathbf{u}(\mathbf{x}_s, t): \mathbb{R}^{n_{sd}+1} \rightarrow \mathbb{R}^{n_{df}}$ to a PDE in residual form accompanied by an initial condition $\mathbf{u}_0(\mathbf{x}_s)$ and Dirichlet boundary conditions $\mathbf{g}(\mathbf{x}_s, t)$, summarized as

$$\text{IBVP} \quad \begin{cases} \mathcal{R}(\mathbf{u}(\mathbf{x}_s, t)) = \mathbf{0}, & \text{on } Q, \\ \mathbf{u}(\mathbf{x}_s, t) = \mathbf{u}_0(\mathbf{x}_s), & \text{at } t = 0, \\ \mathbf{u}(\mathbf{x}_s, t) = \mathbf{g}(\mathbf{x}_s, t), & \text{on } P. \end{cases} \quad (1)$$

While many traditional numerical schemes treat space and time separately, space-time methods, e.g., space-time finite elements [4], have a uniform view on space and time, which is also adopted in physics-informed neural networks for time-dependent problems [5].

2.2 Physics-Informed Neural Networks for a General Initial Boundary Value Problem

The central idea of PINNs is to approximate the solution of an IBVP using a function represented by a neural network [5]

$$\mathbf{u} \approx \hat{\mathbf{u}} := (\mathcal{N}^L(\mathbf{x}; \boldsymbol{\theta}))', \quad \mathcal{N}^L(\mathbf{x}; \boldsymbol{\theta}): \mathbb{R}^{d_{in}} \rightarrow \mathbb{R}^{d_{out}}. \tag{2}$$

Standard feed-forward networks $\mathcal{N}^L(\mathbf{x}; \boldsymbol{\theta})$ (employed in our contribution) consist of L layers of neurons with associated nonlinear activation functions ψ . See Figure 2 for an illustration of a network with two hidden (inner) layers. Connections between the neurons are weighted and all network weights and biases (not pictured in Figure 2) are collected in the parameter vector $\boldsymbol{\theta}$. When solving the forward IBVP (Equation (1)), the network input $\mathbf{x} \in \mathbb{R}^{d_{in}}$ consists of the space-time coordinates, i.e., $d_{in} = n_{sd} + 1$, and the network output represents the degrees of freedom of the considered IBVP, i.e., $d_{out} = n_{df}$. In an extension for a parameterized IBVP, model parameters can be added to the input vector to enable a query of the network prediction for varying parameter values, e.g., when the PINN is used as surrogate model. Model parameters can also be added to the network output to perform parameter identification when additional information is available, e.g., measurement data.

Returning to Equation (2), the network output is not directly used as approximation. Instead, a user-defined transformation $(\cdot)'$ is first applied to the network output. In this contribution, a component-wise output scaling $\hat{\mathbf{u}} = \mathbf{w} \mathcal{N}^L(\mathbf{x}; \boldsymbol{\theta})$, $\mathbf{w} \in \mathbb{R}^{d_{out}}$ is applied to weight the individual contributions. Moreover, the transformation can be used to enforce Dirichlet boundary conditions as hard constraints [6]. The precise form of the transformation can be determined before the network training through inspection of the problem characteristics or found through hyperparameter optimization.

To ensure that the PINN prediction $\hat{\mathbf{u}}$ is a reasonable approximation of the solution \mathbf{u} , the network parameters $\boldsymbol{\theta}$ must be determined according to the IBVP. One can formally state this as optimization problem with a loss function \mathcal{L}_{IBVP} which represents the IBVP

$$\boldsymbol{\theta}^* = \arg \min_{\boldsymbol{\theta}} \mathcal{L}_{IBVP}(\boldsymbol{\theta}), \quad \text{where} \quad \mathcal{L}_{IBVP} = \mathcal{L}_{PDE} + \mathcal{L}_{IC} + \mathcal{L}_{BC}. \tag{3}$$

The individual loss terms can be formulated as *mean squared error*. In the first loss term, the PDE in residual form $\mathcal{R}(\mathbf{u}) = \mathbf{0}$ is transformed into a mean squared error, namely

$$\mathcal{L}_{PDE} = \sum_{i_{df}=0}^{n_{df}} \frac{\hat{w}^{(i_{df})}}{n_{dp}} \sum_{i_{dp}=0}^{n_{dp}} \left[\mathcal{R}^{(i_{df})}(\hat{\mathbf{u}}(\mathbf{x}^{(i_{dp})})) \right]^2. \tag{4}$$

Therein, the inner sum adds up contributions from the n_{dp} data points in the training set, which are used in a sampling-based solution strategy for the optimisation problem (Equation (3)). In the outer sum, the entries of the vector-valued PDE residual \mathcal{R} are weighted by $\hat{w}^{(i_{df})}$ (in addition to the output transformation applied in the construction of $\hat{\mathbf{u}}$). Likewise, violations of the initial and boundary conditions in Equation (1) are transformed into mean squared error loss terms \mathcal{L}_{IC} and \mathcal{L}_{BC} that are evaluated at additional sampling points on the domain boundaries.

When additional information from measurements or simulations is available in form of input-output pairs, respective (weighted) loss terms can be added to the IBVP loss function.

$$\mathcal{L} = \mathcal{L}_{IBVP} + \mathcal{L}_{Simulation\ Data} + \mathcal{L}_{Measurement\ Data}. \tag{5}$$

Such a combination of physics knowledge (IBVP) and available data is a key feature of hybrid digital twins. While the procedure presented in this Section is applicable to general PDE-based IBVPs, we now turn our focus to the specific application case of this contribution.

3 Application Case: Four-Point Bending Test of Reinforced Concrete Beam

As a representative component in civil engineering structures, we consider a steel-reinforced concrete beam. As application case for the hybrid digital twin, the concrete beam is loaded in a four-point bending test configuration as shown in Figure 3 a. The precise experimental setup and details of the data acquisition can be found in the publication of Braml et al. [7]. For the sake of completeness, the most important test case specifications are summarized in the following paragraphs.

The beam has the dimensions $300 \text{ cm} \times b = 15 \text{ cm} \times 30 \text{ cm}$. Positions of the supports and load application points can be seen in Figure 3 b and result in a lever arm $a = 85 \text{ cm}$ (distance between support and load application point). On the (upper) compression side of the beam, steel reinforcement with a cross-sectional area of $A_{S_2} = 1.57 \times 10^{-4} \text{ m}^2$ is placed at a distance $d_2 = 3.9 \text{ cm}$ beneath the beam's top surface. On the tension side, reinforcement with a cross-sectional area of $A_{S_1} = 3.39 \times 10^{-4} \text{ m}^2$ is located at a distance $d_1 = 26.1 \text{ cm}$ beneath the beam's top surface. In the subsequent modeling, a Young's modulus $E_C = 29 \text{ GPa}$ is assumed for the concrete, a Young's modulus $E_S = 200 \text{ GPa}$ is assumed for the construction steel.

To measure longitudinal strains in the beam, fiber-optical sensors are embedded into the concrete in alignment with the reinforcement on compression side (Sensor 1) and on the tension side (Sensor 2). During the considered test a sinusoidal

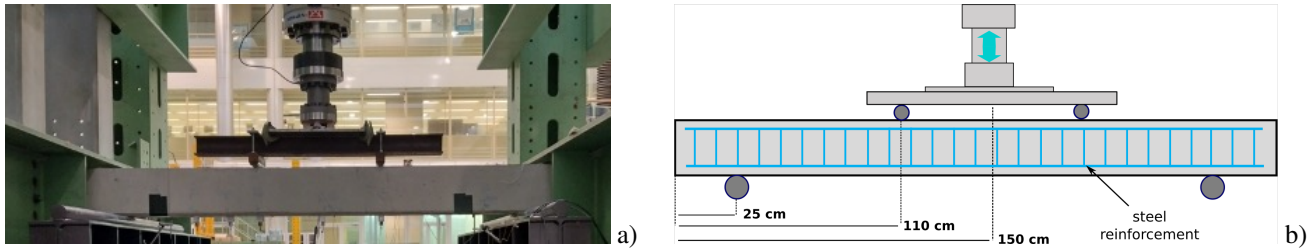


Fig. 3: Four-point bending test of reinforced concrete beam. Picture of the laboratory setup (a) and schematic drawing (b).

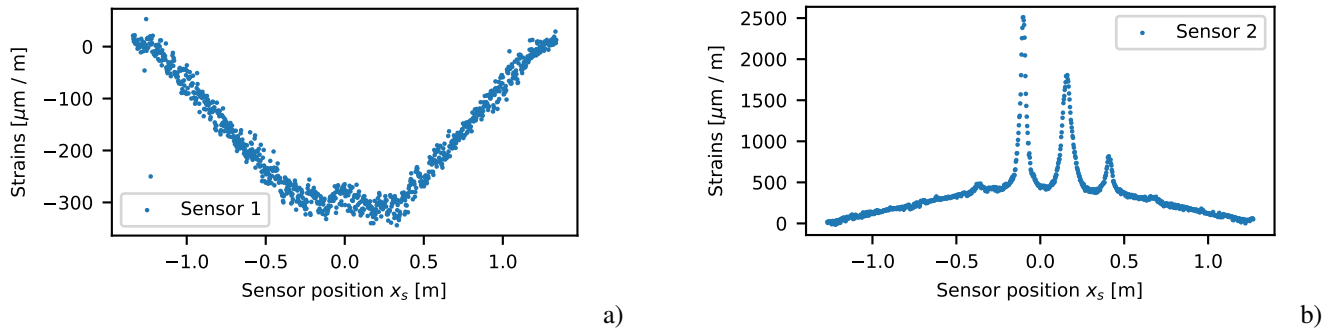


Fig. 4: Fiber-optical strain measurements under the peak load of 10 kN. Compression side on the left (a) and tension side on the right (b).

cyclic load $P(t)$ with a peak value of 10 kN is applied. At a sampling rate of 10 Hz, each fiber-optical sensor reports strain values for approximately 1000 points along the sensor as shown in Figure 4. Despite the alignment of the optical fiber with the steel reinforcements, cracks in the concrete strongly influence the strain measurement on the tension side under the peak load of 10 kN (Figure 4 b). After this outline of the real system, the following section describes its digital representation.

4 Hybrid Digital Twin of Reinforced Concrete Beam

In the following subsections, we present four models to compose a hybrid digital twin of a reinforced concrete beam. The models are ordered according to an increasing model complexity.

4.1 Baseline Model

As BLM, we use a closed-form expression for an estimate of the axial strains in the tension reinforcement, ε_S , provided by civil engineering literature [8, Chapter 5, Section 4.2.1.3]

$$\varepsilon_S = f(E_S, E_C, [a, b, A_{S_1}, A_{S_2}, d_1, d_2], P(t)). \quad (6)$$

The estimate holds for the central region of the beam between the two load application points, where a constant bending moment prevails. Equation 6 omits the explicit (referenced) formula for the estimate, yet stresses the exclusive dependency on material properties, geometric properties, and the applied load as given in Section 3. No model calibration based on the measurement data is performed. In Figure 5, the BLM prediction is compared to the corresponding sensor data and proves to be a reasonable estimate for the bulk strain values. However, this model cannot account for cracks (peaks in the sensor data displayed in Figure 5).

4.2 Data-Driven Model

A model which instead focusses on cracks is explored in the work of Milani et al. [9]. In a first step, the purely data-driven approach approximates a decomposition of the strain measurement into bulk strains and crack influence on the sensor data with an iteratively refined spline fit. After the approximated bulk strain values are subtracted, an outlier analysis is performed to identify data points which can be statistically attributed to a crack. Finally, k-means clustering is applied to the marked data points to find the crack centers. The result of the automatic crack detection in a fiber-optical strain measurement of Sensor 2 is shown in Figure 6.

4.3 Reduced-Order Model: Physics-Informed Neural Network

The combination of physics knowledge and measurement data in one model is tested with a PINN. From the physics point of view, the concrete beam is modeled as elastic continuum. Based on the in-plane loading of the four-point bending test

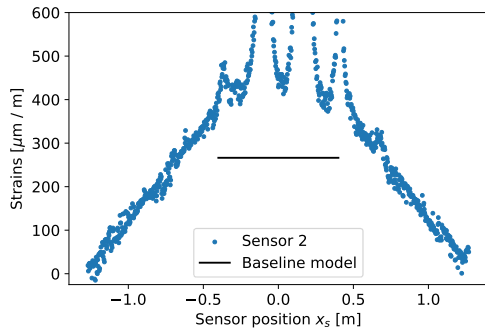


Fig. 5: Baseline model and measurement under the peak load.

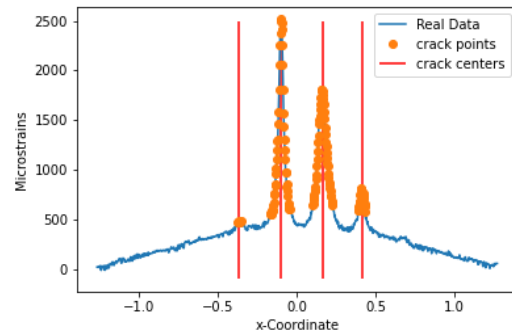
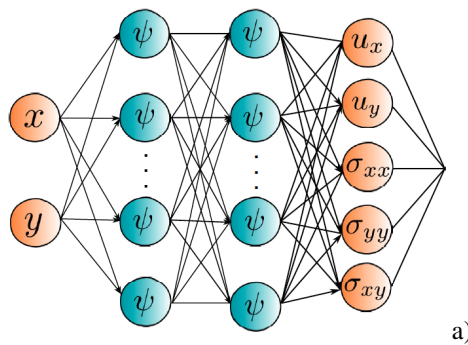
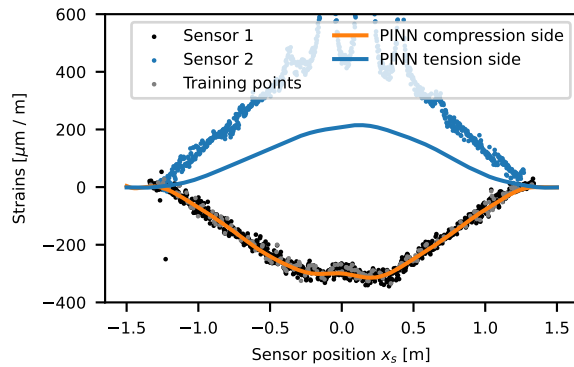


Fig. 6: Crack detection with data-driven model [9].



a)



b)

Fig. 7: Physics-informed neural network. Network architecture visualization (a) and strain prediction (b).

configuration (Section 3), the body is assumed to be in plane-stress state. Hence, it is modeled as two-dimensional linear isotropic elastic continuum in the plane of its major dimensions (as illustrated in Figure 3 b). With this modeling assumption, the influence of the reinforcement can only be considered in a homogenized material model, i.e., as an increased Young’s modulus.

Following the exposition in Section 2.2, the balance equations of linear elasticity in strong form can be directly transformed into a loss function for a PINN. However, preliminary tests showed that a mixed-variable formulation is advantageous compared to a displacement-based formulation. In the employed mixed-variable formulation, the stress tensor components are introduced as additional network outputs as shown in 7 a and mean squared error terms of the constitutive equations are added to the PDE loss (Equation (4)). Moreover, the mixed variable formulation allows for an enforcement of traction boundary conditions as hard constraints [6].

Making use of the available sensor data, 200 data pairs ([position, strain in longitudinal direction]) from the measurement of Sensor 1 (Figure 4 a) are added to the training data set and deviations are included as mean squared error terms in the loss function according to Equation (5). The network training is performed with optimization algorithms provided through the interface of DeepXDE [5].

The trained network can be directly used to predict displacements and stresses at each position of the two-dimensional beam domain. Strain values can be obtained with a simple output operator applied to the network prediction. Figure 7 b compares the network predictions for the sensor positions with the measurement data. On the compression side (Sensor 1), the PINN prediction smoothly interpolates the sensor data. On the tension side (Sensor 2) – where no measurement data was added – the physical model ensures that the PINN predicts roughly the right behavior. Still, the strain values are severely underestimated. In an extension of this work, it is planned to add the magnitude of the load on the beam as an additional network input, to profit from fast network predictions in a parameter-to-solution setting.

4.4 Full-Order Model: Finite Elements

On top of our model hierarchy (with respect to model complexity), we consider a finite element (FE) model which resolves the interaction of reinforcement rods and concrete matrix. To this end, we employ the mixed-dimensional FE framework of Steinbrecher et al. [10, 11]. Namely, the reinforcement rods are discretized with one-dimensional beam elements embedded into a three-dimensional volume mesh of the solid matrix. In preliminary studies, the mixed-dimensional modeling provided a drastic reduction of the computational cost with an acceptable relative accuracy: For the reinforced concrete beam a 3D-3D model has 1 482 648 degrees of freedom, while the 3D-1D model (Figure 8 a) has only 6885 degrees of freedom.

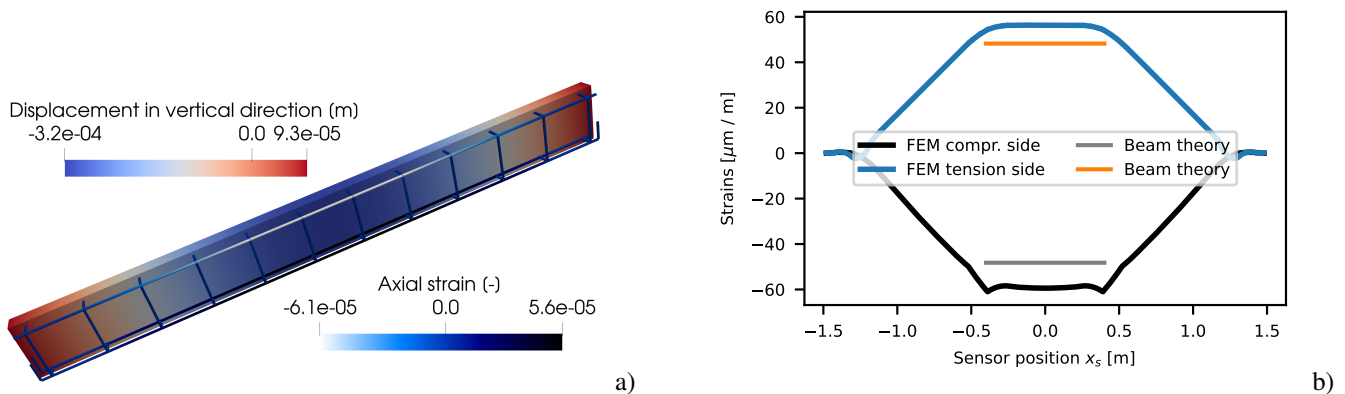


Fig. 8: Finite element model. Reinforcement discretized with beam elements (a). Comparison with linear bending beam theory (b).

The computed displacements of the solid and the axial strains of the beams show that the FE model predicts the behavior of the four-point bending test qualitatively correct (Figure 8 a). However, the use of a linear elastic material model currently prevents the quantitative comparison with measurement data for the concrete beam. Instead, computed strains are compared to a linear bending beam theory estimate which is in reasonable agreement (Figure 8 b).

5 Conclusion and Outlook

We presented a hybrid digital twin concept that incorporates physics knowledge and sensor data of a real physical system. Four models were combined to form a hybrid digital twin for a reinforced concrete beam. The BLM which computes a scalar value for the longitudinal strains in the tension reinforcement is the fastest to evaluate. However, the model relies on a thorough engineering understanding of the physical problem. When less domain knowledge is available, a DDM might help to gain insight from a statistical analysis of the data. Regarding PINNs, we conclude that the method is particularly favorable if measurement data is available and can be added to the loss function of the physical problem formulation. In case of the employed FE model, the effort of combining two advanced modeling techniques (beam-to-solid coupling, material model of concrete) should not be underestimated. In conclusion, a versatile hybrid digital twin contains a model hierarchy which allows to select a model according to the accuracy demands and response-time requirements of the specific query scenario.

Despite the need to further refine the presented methods, steps are taken to address digital twin application cases in the field of critical infrastructures. To this end, sensor data is collected on a 30 m long steel-concrete composite bridge on campus of University of the Bundeswehr Munich. Selected sample data to develop a benchmark study for bridge monitoring is available online at <https://github.com/imcs-compsim/munich-bridge-data>.

Acknowledgements The authors gratefully acknowledge the computing time provided by the Data Science & Computing Lab at University of the Bundeswehr Munich. This research paper is funded by *dtec.bw – Digitalization and Technology Research Center of the Bundeswehr* under the project *RISK.twin*. Open access funding enabled and organized by Projekt DEAL.

References

- [1] Bundesministerium für Verkehr, Bau und Stadtentwicklung, Bauwerksprüfung nach DIN 1076 Bedeutung, Organisation, Kosten, 2013.
- [2] T. Braml, J. Wimmer, Y. Varabei, S. Maack, S. Küttenbaum, T. Kuhn, M. Reingruber, A. Gordt, and J. Hamm, *Bautechnik* **99**(2), 114–122 (2022).
- [3] A. Rasheed, O. San, and T. Kvamsdal, *IEEE Access* **8**, 21980–22012 (2020).
- [4] M. von Danwitz, V. Karyofylli, N. Hosters, and M. Behr, *International Journal for Numerical Methods in Fluids* **91**(0), 29–48 (2019).
- [5] L. Lu, X. Meng, Z. Mao, and G. E. Karniadakis, *SIAM Review* **63**(1), 208–228 (2021).
- [6] L. Lu, R. Pestourie, W. Yao, Z. Wang, F. Verdugo, and S. G. Johnson, *SIAM Journal on Scientific Computing* **43**(6), B1105–B1132 (2021).
- [7] T. Braml, J. Wimmer, and Y. Varabei, *Erfordernisse an die Datenaufnahme und -verarbeitung zur Erzeugung von intelligenten Digitalen Zwillingen im Ingenieurbau (Requirements to data acquisition and processing for the generation of intelligent digital twins in civil engineering)*, in: *Innsbrucker Bautage 2022*, (Studia, 2022).
- [8] A. Albert and K. J. Schneider, *Bautabellen für Ingenieure*, 25 edition (Reguvis, Köln, 2022).
- [9] R. Milani, T. Sahin, M. von Danwitz, M. Moll, A. Popp, and S. Pickl, *Automatic concrete bridge crack detection from strain measurements: a preliminary study*, in: *17th International Conference on Critical Information Infrastructures Security*, Munich, Germany, September 14–16, (2022).
- [10] I. Steinbrecher, M. Mayr, M. J. Grill, J. Kremheller, C. Meier, and A. Popp, *Computational Mechanics* **66**(6), 1377–1398 (2020).
- [11] I. Steinbrecher, A. Popp, and C. Meier, *Computational Mechanics* **69**(3), 701–732 (2022).